Longitudinal Wheel Slip Regulation using Nonlinear Autoregressive-Moving Average (NARMA-L2) Neural Controller

Ryan Christoper R. Dajay[1]
Electronics and Communications Engineering Department
De La Salle University - Manila
Taft Avenue, Manila, Philippines
[1]ryan_christoper_dajay@dlsu.edu.ph

***Abstract* – In this study, the implementation of a nonlinear autoregressive-moving average model (NARMA-L2) neural network controller to maximize the traction of tires during braking scenarios was explored. The proposed controller and system dynamics was done in Simulink. All in all, the neural network controller shows good stability and good response in following the reference trajectory or desired slip ratio. It has experienced the peak worst error of around 2%, its best performance was reached after 89 epochs and it can reach around 99.5% of the reference trajectory or desired slip ratio. Further research should focus on hardware implementation, integration with slip estimation techniques, and, better sets of training data to make the controller more adaptive to different environment and road surface characteristics.**

Keywords – neural controller, slip regulation, NARMA-L2

I. INTRODUCTION

Whenever a vehicle significantly slows down from its intended trajectory, causing it to be unable to reach its predetermined goals, or worse, becomes entrapped without the capability of recovery, the phenomenon of slippage occurs [1]. Slippage is defined as the measurement of lack of progress encountered by the wheels of a vehicle whenever it interacts with its working terrain environment due to either soil displacement or sinkage [2]. Resolving this issue is of high importance for researchers to provide sufficient power distribution to the electrical components of the vehicle, to accomplish expected tasks implemented to the vehicle, and to ultimately optimize the overall performance of the vehicle. Thus, regulating the amount of slippage handled by vehicles becomes an interesting area of research especially in the field of control design.

Various control strategies have been implemented to address the issue of slippage such as model predictive control (MPC), optimal control (OC), and fuzzy logic control (FLC). MPC avoids the possibility of a model-plant mismatch for accurate slip compensation [3]. OC considers the mismatches in path-following scenarios to effectively reduce slippage [4]. FLC provides qualitative relationships among the variables of the system to counteract slipping tendencies [5]. Although these methods suggest promising results, there is need for a controller to adapt with the disturbances presented within the system in a simpler manner.

Artificial-neural-network-(ANN)-based control methods are gaining traction in recent years due to several advantages such as their ability to learn and their simplistic approach to model complex system relationships [6]. Some other notable applications are involved in the field of bioenergy [7], computer vision [8], smart agriculture [9], and swarm robotics [10]. One of the frequently used neural networks for dynamic systems and controls is the nonlinear autoregressive-moving average neural network (NARMA-L2) controller [11]. The core concept of the proposed neural network controller model is to cancel the nonlinearities of the system. In other words, the dynamics of the nonlinear system is approximated to a linear nature [12].

This study aims to design a neural network controller that will maximize traction of the tires during braking conditions to regulate the slip ratio of the angular velocity and longitudinal velocity of a vehicle. Section II will discuss the conceptual framework of the study which includes the dynamics of the vehicle and tires and the design of the neural network controller. Section III will analyze the results derived from the experimentation of the proposed solution. Lastly, Section IV will provide the conclusion and some recommendations for the improvement of the study.

II. CONCEPTUAL FRAMEWORK

A. Vehicle Dynamics

The vehicle dynamics of the system is represented by the quarter car model and tire model as shown in Fig. 1. The relationship between the angular motion and longitudinal motion can be easily seen with the use of a free-body diagram and is described by the set of differential equations presented by equations (1) to (5) [13].

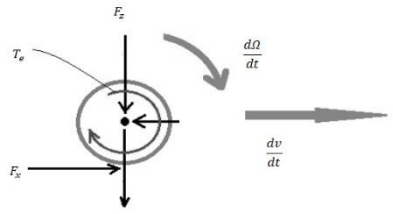

Fig. 1. Free body diagram of a quarter car model in motion

$$J\frac{d\Omega}{d} = R_x - _e \quad (1)$$

$$\frac{d}{d} = -_x \quad (2)$$

$$\lambda = \frac{-r\Omega}{} \quad (3)$$

$$_x = _{zx} \quad (4)$$

$$_z = \quad (5)$$

Equations (1) to (5) will be the basis for the plant model that will be used for the system. An overview of the system consists of the applied wheel torque as our control input signal to achieve our desired slip ratio. Table I provides a summary of the system parameters.

TABLE I. SYSTEM PARAMETERS [14]

Name	Description	Value
Ω	Angular Speed	Calculated
v	Longitudinal Velocity	Calculated
J	Rotational inertia	1 kg m^2
R	Radius	m
T_e	Torque	Input Signal
F_x	Longitudinal Force	Calculated
λ	Longitudinal Slip	Calculated
Fz	Vertical Force	Calculated
μx	Friction Coefficient	Calculated
m	Quarter Vehicle Mass	450 kg
g	Gravitational Force	9.81 m/s^2

B. Tire Dynamics

In tire dynamics, the coefficient of friction experienced by the tire is dependent on several factors such as angular speed, longitudinal speed, the material of the tire, weight experienced by the car and road surface characteristics. Therefore, it is important to include the dynamics of the tire in the development of a slip control mechanism. The tire-road dynamics can be modelled through the use of Pacejka's Magic formula presented in equations (6) and (7) with constant coefficients for longitudinal forces [15].

$$_x = (\lambda, _Z)) = _z \cdot \cdot \sin\delta \quad (6)$$

$$\delta = \arctan\{\lambda - [\lambda - \arctan(\lambda)]\} \quad (7)$$

Coefficients *B, C, D, and E* represent empirical values gathered on different road surface characteristics. For this study, the road surface condition considered is dry asphalt. F_z *and* λ represents the vertical load and the slip ratio respectively.

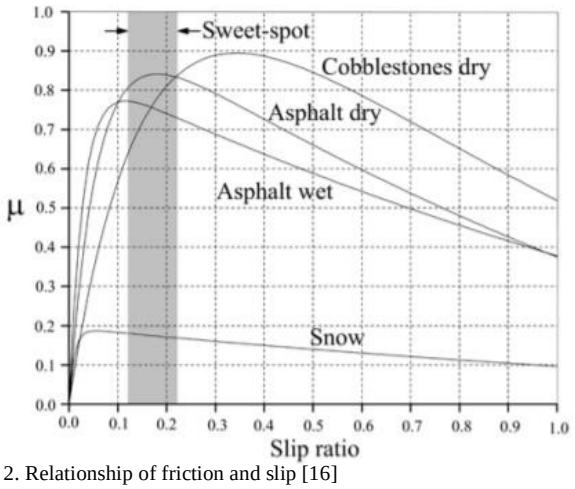

Fig. 2. Relationship of friction and slip [16]

Fig. 2 shows the relationship of slip and the coefficient of friction experienced by the tire [16]. From the graph, the amount of friction experienced by the tire changes with respect to the difference between its angular speed and longitudinal speed, or, its slip ratio. An interesting part of graph is shown in the grey-shaded area called the *'the sweet spot'*. The grey shaded area or *'sweet spot'* is an interesting phenomenon where the coefficient of friction occurs at its maximum, and, in other words, the frictional force is also at its maximum. An important design factor seen in anti-lock braking systems is to regulate the amount of slip ratio of the car. Typically, the desired amount for most road surface is between *5%-20%* as this provides the maximum frictional coefficient and frictional force. This provides the least time spent in braking and allows the vehicle to be steered [17].

C. Design of Neural Network Controller

The design of the NARMA-L2 controller consists of two steps namely: the identification of the system to be controlled and design of the system control [18]. In the system identifications stage, the forward dynamics of the system is represented by a neural network. And, the general discrete-time nonlinear system is approximated through the use of the nonlinear autoregressive-moving average (NARMA) model as seen in the equation (8) where *u(k)* is the system input, *y(k)* is the system output, and, *m* and *n* are the input and output delay values respectively.

$$y(k+d) = N[y(k), y(k-1), \dots, y(k-n+1), u(k), u(k-1), \dots, u(k-n+1)] \quad (8)$$

Furthermore, the output of the system can follow a set reference trajectory $y(k+d) = y_r(k+d)$ that will yield to a nonlinear controller given by the equation (9)

$$u(k) = G[y(k), y(k-1), \dots, y(k-n+1), y_r(k+d), u(k-1), \dots, u(k-m+1)] \quad (9)$$

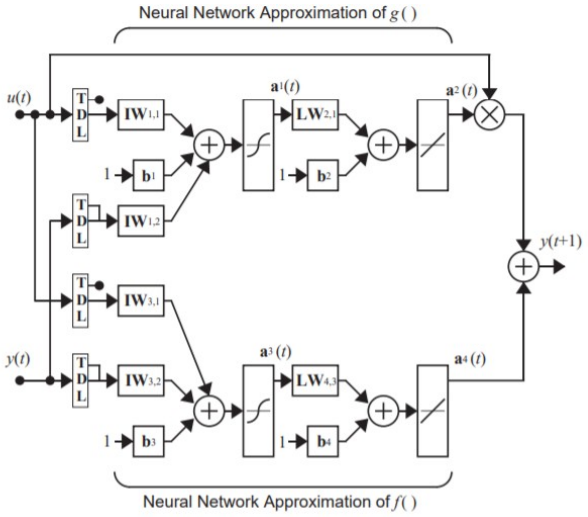

Fig 3. Architecture of nonlinear autoregressive-moving average model neural network

Fig. 3 shows the neural netwok architecture of the equation (9) or nonlinear-autoregressive moving average model. It can be seen that the functions *f( ) and g( )* are approximated through the use of two neural networks. However, the nonlinear controller yielded above can be quite slow because dynamic backpropagation will be the optimization algorithm used to minimize the mean square error for approximating function *G*. Instead of using the NARMA model discussed above, the NARMA-L2 [11] is considered to approximate the system which will yield to the equation (10) below.

$$\begin{aligned} y(k+d) = f[&y(k), y(k-1), \dots, y(k-n+1), u(k \\ &-1), \dots, u(k-m+1)] \\ &+ g[y(k), y(k-1), \dots, y(k-n \\ &+1), u(k-1), \dots, u(k-m+1)] \\ &\cdot u(k) \end{aligned} \tag{10}$$

The control input *u(k)* needed for the system output to follow the reference trajectory $y(k+d) = y_r(k+d)$ can be easily determined by rearranging the previous equation which will yield to the equations (11) to (13) presented below.

$$u(k) = \frac{NUM}{DEN} \tag{11}$$

$$= y\ (k+,d) - [y(k), y(k-1), \dots, y(k- \\ +1), (k-1), \dots, (k- +1)] \tag{12}$$

$$= [y(k), y(k-1), \dots, y(k- +1), (k \\ -1), \dots, (k- +1)] \tag{13}$$

The problem with the previous equation that it can't be used directly to determine the control input *u(k)* based on the output at the same time *y(k)* which causes realization problems. Instead of this, the following equation model presented in equation (14) should be used to determine the control input *u(k)* based on the output at the same time *y(k).*

$$\begin{aligned} y(k+d) = f[&y(k), y(k-1), \dots, y(k-n+1), u(k \\ &-1), \dots, u(k-n+1)] \\ &+ g[y(k), y(k-1), \dots, y(k-n \\ &+1), u(k-1), \dots, u(k-n+1)] \\ &\cdot u(k) \end{aligned} \tag{14}$$

Following the system identification stage is the design of the system control. Fig. 4 below shows how the NARMA-L2 controller is implemented in a control system environment. The plant block represents the dynamic model of our system. The controller block consist of the NARMA-L2 controller; and, the reference model is the reference trajectory or desired setpoint to achieve our desired system response.

For this study, the plant block represents the dynamics of the vehicle. The control input signal is the applied wheel torque to the wheel. And the output signal is the calculated slip through determination of current angular velocity and current longitudinal velocity. The reference model or reference trajectory is the desired slip of the system. That being said, the neural network controller will vary the control input signal to make the output signal follow our desired reference trajectory. Fig. 5 shows the NARMA-L2 model with the neural controller implemented in the design.

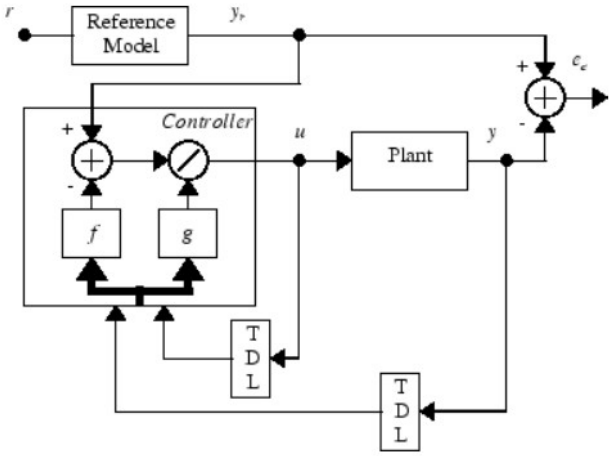

Fig. 4. Block diagram of NARMA-L2 control system [11]

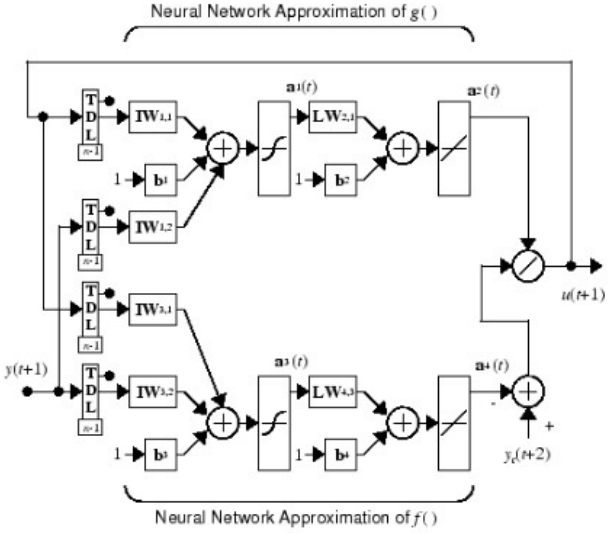

Fig. 5. Neural network controller with NARMA-L2 model [18]

III. ANALYSIS OF RESULTS

The NARMA-L2 controller was first trained by forming a dataset through generating random samples of the plant input and its corresponding plant outputs. A total of *1000* samples were generated to train the neural network controller. Furthermore, the neural network controller was trained using the Levenberg-Marquadt backpropagation algorithm, or also known as the damped-least squares method. The algorithm has a fast and stable convergence and is most suitable for non-linear systems [19].

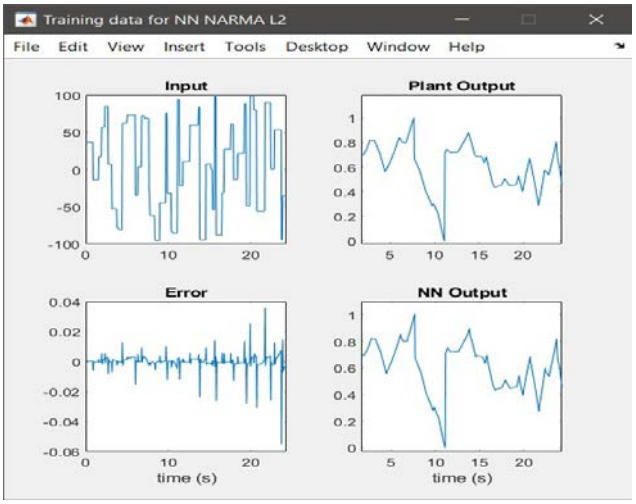

Fig. 6. Training data for NARMA-L2 neural controller

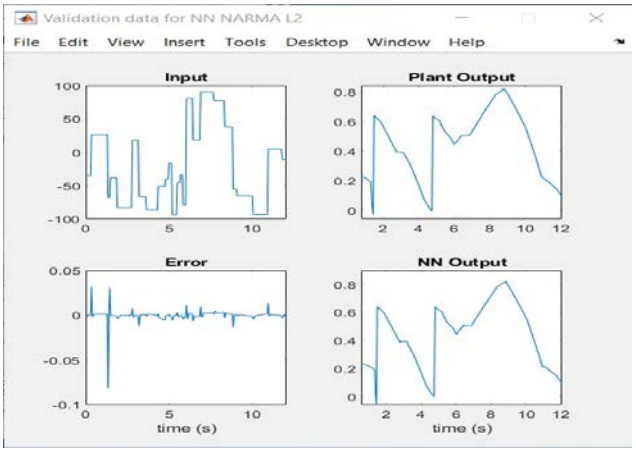

Fig. 7. Validation data for NARMA-L2 neural controller

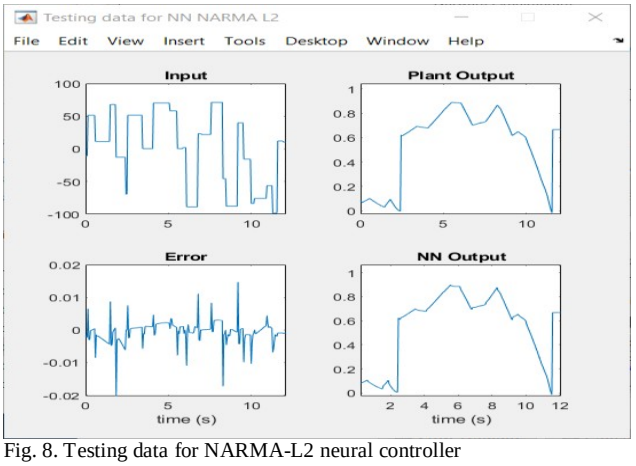

Fig. 8. Testing data for NARMA-L2 neural controller

Fig. 6, Fig. 7, and Fig. 8 present the corresponding performance of the neural network controller. By looking at the graphs of the neural network performance, it can be seen that the neural network controller experiences a peak worst error of around *2%*.

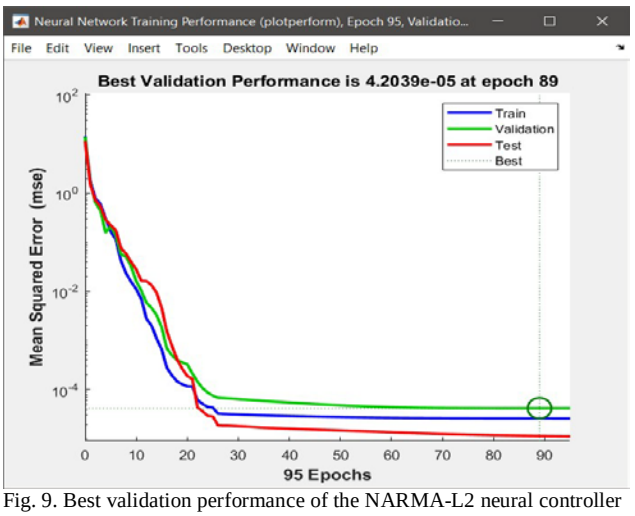

Fig. 9. Best validation performance of the NARMA-L2 neural controller

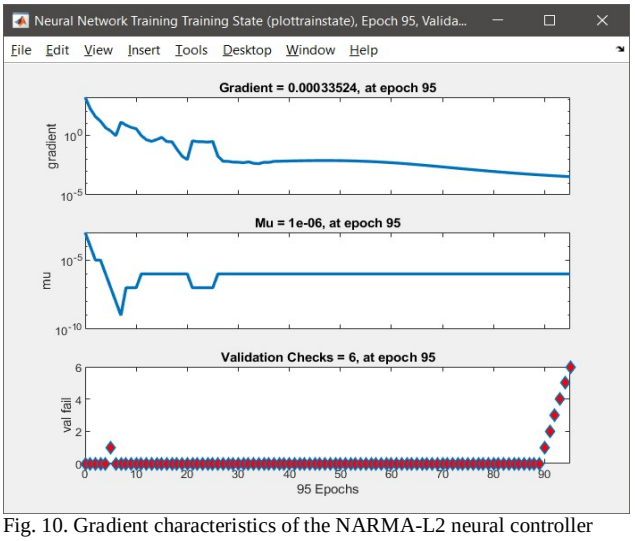

Fig. 10. Gradient characteristics of the NARMA-L2 neural controller

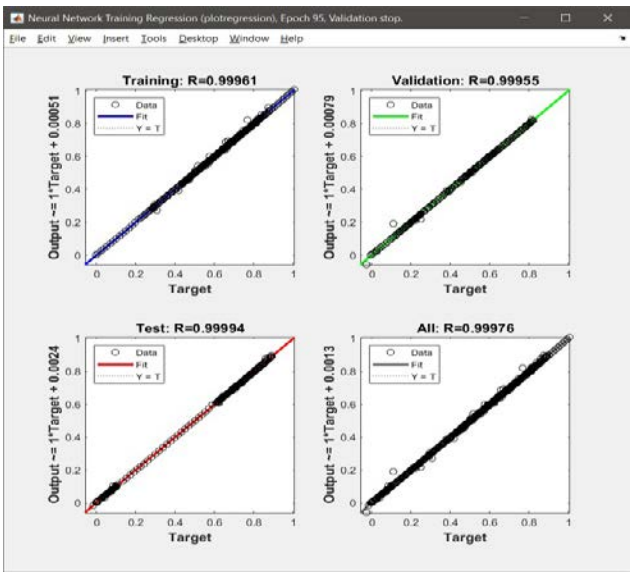

Fig. 11. Regression characteristics of the NARMA-L2 neural controller

Fig. 9, Fig. 10, and Fig. 11 display that the neural network controller's root mean squared error is reduced per epoch. An epoch is defined as one forward pass and one backward pass of all the training examples. The best performance for our neural network controller was achieved after *89* epochs. Also, seen in the graph are the other important training statistics such as the gradient and regression properties of the neural network.

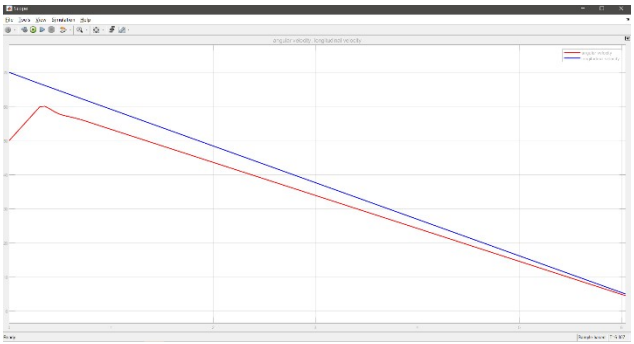

Fig. 12. Longitudinal velocity and angular velocity response of the system

Fig. 12 shows the time response of the system's longitudinal and angular velocity under braking conditions and initially the longitudinal velocity and angular velocity are not matched. The angular velocity is being controlled to have a desired slip ratio by varying the applied torque to the wheel. As discussed previously, the maximum frictional force happens averagely in the range of *5% - 20%*. For the tests done, the desired slip ratio or reference trajectory was set around to *10%* or *0.1* as it is the slip ratio that will maximize traction for dry asphalt road conditions.

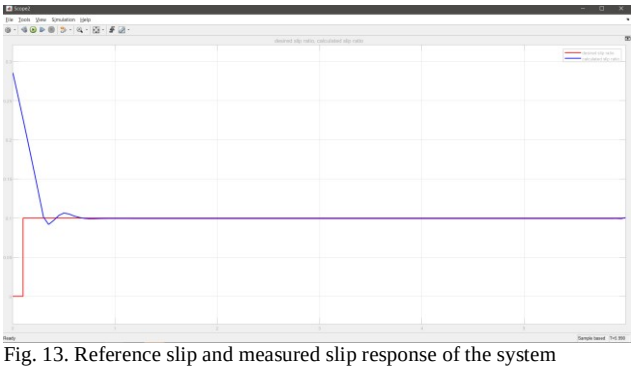

Fig. 13. Reference slip and measured slip response of the system

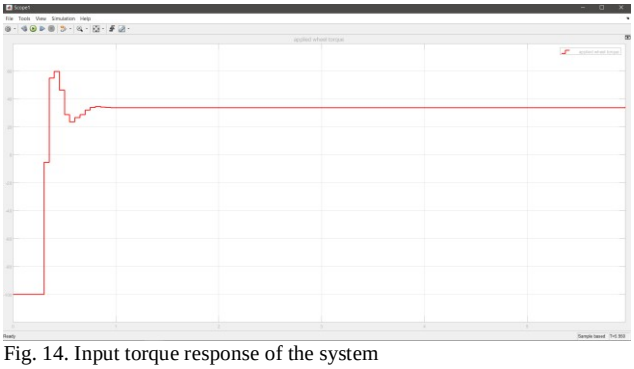

Fig. 14. Input torque response of the system

From Fig. 12 and Fig. 13, the neural network controller displays a very smooth and fast response to the desired slip ratio or reference trajectory. Furthermore, the response of the controller shows minimal oscillations during transient and no oscillations were found during steady-state response. It was measured the present neural network controller can only reach around *0.995* or *99.5%* of the reference trajectory or desired slip ratio. This means that the controller has an error of around *0.5%*. Fig. 14 shows the input signal torque and how it is being varied to follow the reference trajectory or desired slip ratio. Fig. 15 presents the side-by-side graph of all relevant responses in the system.

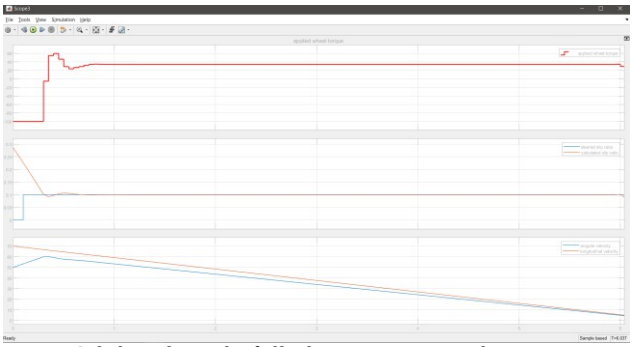

Fig. 15. Side-by-side graph of all relevant responses in the system

IV. CONCLUSIONS AND RECOMMENDATIONS

In conclusion, the nonlinear autoregressive-moving average model (NARMA-L2) neural controller was successfully implemented for slip control to maximize traction for the tires especially during braking scenarios. The designed controller was able to follow closely the desired reference trajectory. From the gathered data, the neural network controller shows good stability and has a good response in following the reference trajectory or the desired slip ratio. However, the neural network controller's accuracy to the reference trajectory can still be improved with better sets of training data and its performance can be improved with other training algorithms.

Furthermore, the research about slip control is important as it is largely used in the fields of anti-lock braking systems which contributes to the vehicles overall safety. And, improving the performance of vehicles by reducing power consumption, time, and distance spent in braking through slip regulation.

On the other hand, slip control is also being implemented in unmanned ground vehicles to prevent the vehicles from being damaged and to lower the risk of entrapment. Slip control is also used to help the unmanned ground vehicles to traverse difficult areas such as inclined and uneven terrains.

There are still a lot possible developments in this area of research. One possible direction is the hardware implementation of the neural controller. The performance of the said controller should be tested extensively and a comparison study should be done with other existing controllers. Second, the training of the neural network can also be improved to accommodate different road surface characteristics and to have better controller accuracy and response. In order to do that, multiple datasets involving different scenarios, environments, and road surface

characteristics should be gathered to improve the controller's robustness and adaptability. Different learning algorithms should also be explored to help reduce the error of the neural network. Third, the integration of slip estimation techniques with slip control techniques should be explored especially in a hardware set-up. Lastly, research about slip control including both lateral slip and longitudinal is another potential area of research.

ACKNOWLEDGMENT

The proponents would like to extend their gratitude to the Department of Science and Technology – Engineering Research and Development for Technology (DOST-ERDT) program for making this research possible.

REFERENCES

[1] A. Angelova, L. Matthies, D. Helmick and P. Perona, "Learning and Prediction of Slip from Visual Information," *Journal of Field Robotics*, vol. 24, no. 3, 2007.

[2] R. Gonzalez and K. Iagnemma, "Slippage estimation and compensation for planetary exploration rovers. State of the art and future challenges.," *Journal of Field Robotics*, vol. 35, no. 4, pp. 1-14, 2017.

[3] M. Burke, "Path-Following Control of a Velocity-Constrained Tracked Vehicle Incorporating Adaptive Slip Estimation," in *IEEE International Conference on Robotics and Automation*, Saint Paul, MN, USA, 2012.

[4] V. Rajagopalan, C. Mericli and A. Kelly, "Slip-Aware Model Predictive Optimal Control for Path Following," in *IEEE International Conference on Robotics and Automation*, Stockholm, Sweden, 2016.

[5] C. Geng, L. Mostefai, M. Denai and Y. Hori, "Direct Yaw-Moment Control of an In-Wheel-Motored Electric Vehicle Based on Body Slip Angle Fuzzy Observer," *IEEE Transactions on Industrial Electronics*, vol. 56, no. 5, pp. 1411-1419, 2009.

[6] O. I. Abiodun, A. Jantan, A. E. Omolara, K. V. Dada, N. A. Mohamed and H. Arshad, "State-of-the-art in artificial neural network applications: A survey," *Heliyon*, vol. 4, no. 11, pp. 1-41, 2018.

[7] A. P. Mayol, J. M. Maningo, A. G. A. Chua-Unsu, C. Felix, P. Rico, G. Chua, E. Manalili, D. Fernandez, J. Cuello, A. Bandala, A. Ubando, C. Madrazo, E. Dadios and A. Culaba, "Application of Artificial Neural Networks in Prediction of Pyrolysis Behavior for Algal Mat (LABLAB) Biomass," in *IEEE 10th International Conference on Humanoid, Nanotechnology, Information Technology, Communication and Control, Environment and Management*, Baguio City, Philippines, 2018.

[8] R. A. R. Bedruz, A. H. Fernando, A. A. Bandala, E. Sybingco and E. P. Dadios, "Vehicle Classification Using AKAZE and Feature Matching Approach and Artificial Neural Network," in *2018 IEEE Region 10 Conference (TENCON 2018)*, Jeju, South Korea, 2018.

[9] J. C. Puno, E. Sybingco, E. Dadios, I. Valenzuela and J. Cuello, "Determination of Soil Nutrients and pH level using Image Processing and Artificial Neural Network," in *IEEE 9th International Conference on Humanoid, Nanotechnology, Information Technology, Communication and Control, Environment and Management*, Manila, Philippines, 2017.

[10] J. M. Z. Maningo, G. E. U. Faelden, R. C. S. Nakano, A. A. Bandala and E. P. Dadios, "Obstacle Avoidance for Quadrotor Swarm Using Artificial Neural Network Self-Organizing Map," in *2015 International Conference on Humanoid, Nanotechnology, Information Technology, Communication and Control, Environment and Management*, Cebu City, Philippines, 2015.

[11] R. Celikel and O. Aydogmus, "NARMA-L2 Controller for Single Link Manipulator," in *International Conference on Artificial Intelligence and Data Processing*, Malatya, Turkey, 2018.

[12] A. Pukrittayakamee, O. De Jesus and M. T. Hagan, "Smoothing the Control Action for NARMA-L2 Controllers," in *2002 45th Midwest Symposium on Circuits and Systems*, Tulsa, OK, USA, 2002.

[13] R. Rajamani, Vehicle Dynamics and Control (Second Edition), Springer US, 2012.

[14] A. A. A. Emheisen, A. A. Ahmed, N. I. Alhusein, A. A. Sakeb and A. S. Abdulhamid, "Car Wheel Slip Modelling, Simulation, and Control using Quarter Car Model," *International Journal of Engineering Trends and Technology (IJETT)*, vol. 28, no. 6, pp. 291-293, 2015.

[15] H. B. Pacejka, Tyre and Vehicle Dynamics (2nd Edition), London, United Kingdom: Butterworth-Heinemann, 2006.

[16] M. H. Khansari, M. Yaghoobi and A. Abaspour, "Independent Model Generalized Predictive Controller Design for Antilock Braking System," *International Journal of Computer Applications*, vol. 114, no. 1, pp. 18-23, 2015.

[17] T. Bera, K. Bhattacharya and A. Samantaray, "Evaluation of antilock braking system with an integrated model of full," *Simulation Modelling Practice and Theory*, vol. 19, pp. 2131-2150, 2011.

[18] M. T. Hagan, H. B. Demuth, M. H. Beale and O. De Jess, Neural Network Design, Martin Hagan, 2014.

[19] B. M. Wilamowski and H. Yu, "Improved Computation for Levenberg-Marquardt Training," *IEEE Transactions on Neural Networks*, vol. 21, no. 6, pp. 930-937, 2010.